3D holographic printer: Fast printing approach

Alexander V. Morozov, [1,*] **Andrey N. Putilin,** [2] **Sergey S. Kopenkin,** [3] **Yuriy P. Borodin,** [3] **Vladislav V. Druzhin,** [1,4] **Sergey E. Dubynin** [1] **and German B. Dubinin** [1]

[1] *SAIT Russia Lab, Samsung R&D Institute Rus, 2013 Office 1501, bldg.1, 12, Dvintsev str., Moscow 127018, Russia*
[2] *P.N. Lebedev Physical Institute of the Russian Academy of Sciences, 53, Leninskiy Prospect, 119991, Moscow, Russia*
[3] *Moscow State Technical University of RadioTechnics, Electronics and Automatics, 78, Vernadskogo ave., 119454, Moscow, Russia*
[4] *Moscow State Technical University n.a. Bauman, bldg.1, 5, 2-ya Baumanskay str., Moscow 105005, Russia*
[*] *alexander.morozov@samsung.com*

Abstract: This article describes the general operation principles of devices for synthesized holographic images such as holographic printers. Special emphasis is placed on the printing speed. In addition, various methods to increase the printing process are described and compared.

OCIS codes: (210.2860) Holographic and volume memories; (230.3120) Integrated optics devices; (230.7370) Waveguides.

References and links

1. S.A. Benton, V.M. Bove Jr., *Holographic Imaging* (Wiley-Interscience, 2008), 1st ed.
2. H. Kogelnik, "Couple wave theory for thick hologram gratings," Bell System Technical Journal **48**, 2909–2949 (1969).
3. Michael Klug, Mark Holzbach, Alejandro Ferdman, "Method and apparatus for recording one-step, full-color, full-parallax, holographic stereograms," (2001). US patent 6330088 B1, Dec. 11, 2001.
4. David Brotherton-Ratcliffe, Stanislovas J. Zacharovas, Ramunas J. Bakanas, Julius Pileckas, Andrej Nikolskij, Jevgenij Kuchin, "Digital holographic printing using pulsed RGB lasers," Opt. Eng. **50(9)**, 091307 (August 03, 2011).
5. Craig Newswanger, Pankaj Lad, Robert L. Sitton, Qiang Huang, Michael A. Klug, Mark E. Holzbach, "Pulsed-laser systems and methods for producing holographic stereograms," (19-Oct.-2004). US 6806982 B2.
6. Michael J. Kidger, *Fundamental Optical Design* (Society of Photo Optical, 2002).
7. Equation (2) is written in the square hogel form.
8. Keehoon Hong, Soon-gi Park, Jiwoon Yeom, Jonghyun Kim, Ni Chen, Kyungsuk Pyun, Chilsung Choi, Sunil Kim, Jungkwuen An, Hong-Seok Lee, U-in Chung, Byoungho Lee, "Resolution enhancement of holographic printer using a hogel overlapping method," Opt. Express **21**, 14047–14055 (2013).
9. David Brotherton-Ratcliffe, Florian Michael Robert Vergnes, Alexey Rodin, Mikhail Grichine, "Holographic printer," (2005). US patent 6930811 B2, Aug. 16, 2005.
10. Equation (6) is written for the case when the speed of the material is the same in each direction.
11. H.I. Bjelkhagen, "Silver Halide Recording Materials for Holography and Their Processing," Springer Series in Optical Sciences, Vol. **66** (Springer-Verlag, Heidelberg, New York 1993).
12. Friedrich-Karl Bruder, Francois Deuber, Thomas Fcke, Rainer Hagen, Dennis Hnel, David Jurbergs, Thomas Rlle, Marc-Stephan Weiser, "Reaction-diffusion model applied to high resolution Bayfol HX photopolymer," Proceedings of SPIE **7619**, 76190I-76190I-15 (2010).
13. Horst Berneth, Friedrich-Karl Bruder, Thomas Fcke, Rainer Hagen, Dennis Hnel, Thomas Rlle, Gnther Walze, Marc-Stephan Weiser, "Holographic recordings with high beam ratios on improved Bayfol HX photopolymer," Proceedings of SPIE **8776**, 877603-877603-12 (2013).

#200122 - $15.00 USD Received 24 Oct 2013; revised 13 Dec 2013; accepted 15 Dec 2013; published 27 Jan 2014

14. Viktor N. Mikhailov, K. T. Weitzel, Vitaly N. Krylov, Urs P. Wild, “Pulse hologram recording in dupont’s photopolymer films,” Proc. SPIE **3011**, 200–202 (1997).
15. Viktor N. Mikhailov, K. T. Weitzel, Tatiana Y. Latychevskaia, Vitaly N. Krylov, Urs P. Wild, “Pulse recording of slanted fringe holograms in dupont photopolymer,” Proceedings of SPIE **3294**, 132–135 (1998).
16. H.J. Caulfield, *Handbook of Optical Holography* (Academic Press, 1980).
17. The coefficient 2 before root sign takes into account the situation when the acceleration and deceleration are equal.
18. In our experimental setup we are using 4F optical system to be able to simple modify it for implementing different multi-hogel printing techniques.
19. Kyungsuk Pyun, Chilsung Choi, Alexander Morozov, Sunil Kim, Jungkwuen An, Hong-seok Lee, Uni Chung, “Integrated Hologram Optical Head for Holographic Printer,” in Digital Holography and Three-Dimensional Imaging, OSA Technical Digest (online), Optical Society of America (2013), paper DW4A.2.
20. Note that, the total exposure time has not changed. However, the time required to record one hogel will depend on the number of simultaneous recorded hogels and will be equal to $\tau M^2 = d^2 \frac{S}{P\varepsilon} M^2$. Therefore, the required waiting time must be increased because of the increased single hogel exposure time. It is impossible to define the changes in the waiting time because it depends on the real exposure time, wavelength, and rigidity of the entire system. As such, in the future, we will not take into account the waiting time changes, which is true for very short exposure times as well as a low M.
21. Andrew N. Putilin; Alexander V. Morozov; Ivan V. Bovsunovskiy, “Optical device with Fourier transforming optical components for one step multi-micro-hologram recording using wedge system,” (2012). Russian Patent Application RU 2012127529, July 03, 2012.
22. Eqs. (15), (17), and (19) are true for the case for the field of view of a synthesized holographic image recorded using the single hogel printing technique and is equal to the field of view of the image recoded using the spatial hogel spectra splitting technology if and only if both designs used the same SLM.
23. The maximum permissible value of the numerical aperture for the Fourier transforming system containing a large linear field was 0.76.
24. For simplicity, a SLM with a pixel number equal to N and an aspect ratio of 1:1 is used.
25. Andrew N. Putilin; Alexander V. Morozov; Ivan V. Bovsunovskiy, “Optical device with multi aperture Fourier transforming optical components for one step multi-micro-hologram recording,” (2012). Russian Patent Application RU 2012120356, May 17, 2012.
26. In the above calculations, the exposure time (τ), moving time (t_{move}), waiting time (t_{wait}), and time for scheme shift (t_{shift}) are 0, 10, 50, and 5 ms, respectively. The maximum numerical aperture of the Fourier transforming optical system was set to 0.76.

1. Introduction

The visualization of the 3D reality is one of the most complicated problems of modern applied optics because of the giant data flux and phenomenal visual abilities of human eyes both. Holography as a general 3D information reconstruction method permits to develop the required display, however, the main disadvantage of holography is that it is essential to use real objects during hologram recording. In [1], Stephen Benton proposed a point-by-point method of synthesizing holographic images, which allows to overcome this disadvantage. Holographic printers are one of most promising devices capable of solving the problem of synthesizing combined real 3D and virtual objects. Reference and signal beams are used to produce interference inside a light-sensitive material but the recording is local and the recording process is a point-to-point recording of general interference pattern.. In addition, high diffraction efficiency can be achieved using the Bragg diffraction created by volume phase holographic gratings [2].

2. Principle of holographic printer

Figure 1 shows a schematic diagram of the holographic printer proposed by Stephen Benton. The numerous schemes proposed later have a little changes in the general principles of hologram synthesis (e.g. in [3–5]). Principle design consists of several core elements: a coherent light source (laser), beam splitter, spatial light modulator, Fourier transforming optical system, reference beam forming optical system, and light sensitive material for micro-hologram recording. The data from a plurality of Fourier micro-hologram is recorded using the operation principle described by Stephen Benton. Each micro-hologram allows for the reconstruction of

#200122 - $15.00 USD Received 24 Oct 2013; revised 13 Dec 2013; accepted 15 Dec 2013; published 27 Jan 2014

the spatial spectrum that corresponds to illumination of the recording object, which should pass through that particular point in light sensitive material. For this case, the printed hologram is a quantized holographic stereoscopic image of the object. The spatial spectrum of each micro-hologram is defined by the amplitude modulation of the signal beam due to the spatial light modulator. The required angular spatial spectrum of each element of the synthesized image is formed by the amplitude modulated light that passed through the Fourier transforming optical system.

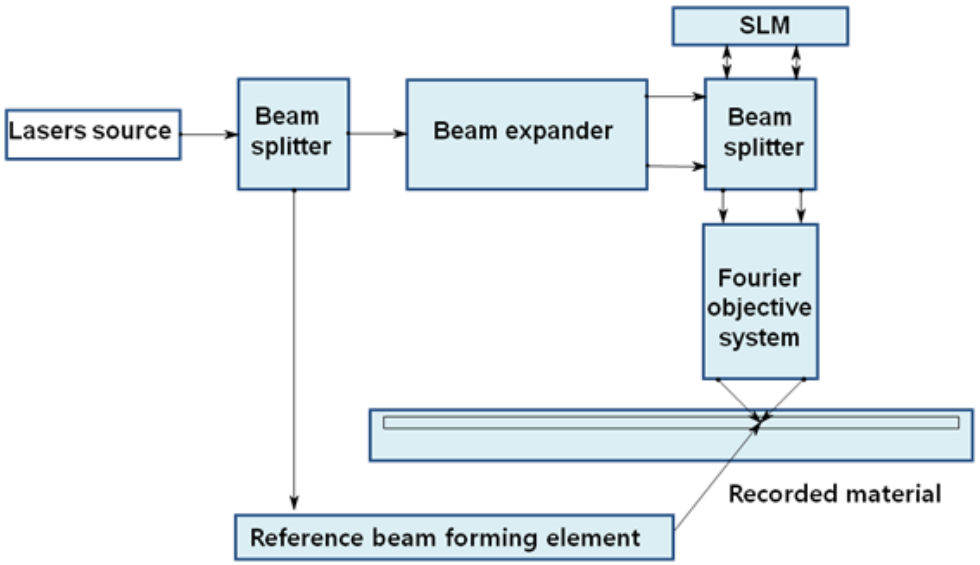

Fig. 1. Schematic diagram showing the main design of the holographic printer proposed by Stephen Benton.

Each micro-hologram is recorded using the classical holographic method, which contains reference and signal beams. Volume holographic mediums are used as the light sensitive material for a convenient observation of the recorded image in white light conditions. Such holographic mediums allow us to record volume phase gratings with a high spatial and spectral selectivity.

3. Quality of synthesized holographic image

When a continuous holographic image is represented separately as spatial and information elements, a reduction in the quality of the demonstrated image occurs. It is known that the human eye has 1-2 arc minutes of angular resolution ($\delta\gamma$). In accordance with Eq. (1), the maximum size of an element in a holographic image (hogel) should be less than 300 μm with the observation distance (l) equal to 300 mm

$$d_{max} \leq 2l \tan \frac{\delta\gamma}{2}. \tag{1}$$

Moreover, according to [6] a reduction in the hogel size leads to a reduction in the angular resolution of the synthesized image given by [7]

$$\Delta\gamma = \arctan \frac{\lambda}{\alpha d}, \tag{2}$$

#200122 - $15.00 USD Received 24 Oct 2013; revised 13 Dec 2013; accepted 15 Dec 2013; published 27 Jan 2014

where d, λ, and α represent the hogel size, wavelength of the reconstructing light radiation, and aberration coefficient, respectively. The estimated reduction of the angular resolution is a consequence of the synthesized image of the Fourier transforming optical system spatial spectrum formation.

Equation (2) makes it possible to determine an equation for the minimum hogel size

$$d_{min} \geq \frac{\lambda}{\alpha \tan \Delta\gamma}. \tag{3}$$

In general, in order to produce a good quality hologram, the angular resolution must equal 0.5°. Moreover, for an aberration-free optical system, i.e., $\alpha = 1.0$, the minimal acceptable hogel size (d_{min}) must be equal to 61 μm for the reconstructing light radiation of $\lambda = 0.532$ μm.

Thus, the size of a single hogel for the standard parameters of the synthesized image observation is limited by range and can be determined using

$$\frac{\lambda}{\alpha \tan \Delta\gamma} \leq d \leq 2l \tan \frac{\delta\gamma}{2}. \tag{4}$$

In [8], Keehoon Hong et al. a new method is proposed to partially solve the hogel spatial and angular resolution contradiction that is limited by (4). However, that method requires the use of overlapping hogels, which dramatically increases the printing time.

4. Printing speed

While recording holograms, one of the major problems that a researcher encounters is the effects of vibrations on the diffraction efficiency of the recording grating. Moreover, the requirements for an acceptable level of vibration are difficult to fulfill as the spatial frequency that is used to form interference patterns is increased. In accordance with (4), there are two basic ways to print synthesized holographic images: printing on a continuously moving material (continuous printing) and printing with periodic stops (step-by-step printing).

4.1. Continuous printing

Implementing micro-holograms recordings on a continuously moving material requires a coherent radiation source such as a pulsed laser capable of producing very short exposure times. There have been many investigations describing devices with pulsed laser sources [3, 4, 9]. Common pulsed lasers have pulse durations ranging from a few *ps* to tens of *ns* and produce a few *mJ* of energy. Therefore, as the energy of the generated pulse is increased, the volume of the laser active media also increases, while the pulse repetition frequency (f_{pulse}) decreases. The minimum printing time, T, can be determined using

$$T \geq \frac{A}{d^2 f_{pulse}}, \tag{5}$$

where A, d, and f_{pulse} represent the total printing area, size of one hogel, and pulse repetition frequency, respectively.

Conversely, the maximum printing time depends on the speed of the material [10]

$$T \leq \frac{A}{dv}, \tag{6}$$

where v represents the speed of the material.

#200122 - $15.00 USD Received 24 Oct 2013; revised 13 Dec 2013; accepted 15 Dec 2013; published 27 Jan 2014

In accordance with Eqs. (5) and (6), the printing time for a single sample is limited by the expression

$$\frac{A}{d^2 f_{pulse}} \leq T \leq \frac{A}{dv}. \tag{7}$$

Furthermore, the pulsed printing imposes additional restrictions on the type of light-sensitive recording material. Currently, the most commonly used materials are silver halide emulsion and photopolymer materials. The characteristics of these materials are shown in Table 1 according to [11–13].

Table 1. Common characteristics of photopolymers and silver halide.

	Photopolymer	**Silver Halide**
Toxic	No	Yes
DE, %	~ 99	~ 50
Sensitivity, $\frac{mJ}{cm^2}$	$1 \sim 1000$	$0.01 \sim 1$
Post Process	Dry	Wet
In-situ recording	Yes	No
Thick film	Yes	No
Response time	μs	ps

As can be seen from Table 1, the photopolymer materials have a number of advantages from the consumer viewpoint, i.e., they are non-toxic, do not require a wet developer, can restore the image immediately after recording, and thicker material layers are possible. These thicker layers have a positive effect on the spectral and spatial selectivity of the formed gratings. Conversely, the silver halide materials allow for very short exposure times, i.e., a few *ps*, and exhibit a higher sensitivity compared to the photopolymer materials.

Many researchers have considered the application of pulse recording on photopolymer materials [5, 14, 15]. In particular, Mikhailov et al. discovered the possibility of using pre-exposed materials before the pulse recording. However, this method does not reduce the energy required for the formation of a holographic grating [14, 15]. Additionally, this approach requires the creation of special optical devices for preliminary local exposures of the material. Meanwhile, in [5], Craig Newswanger et al. is discussed approach which uses the multi-exposure method, and the total energy required to form the grating is divided into multiple pulses with a defined impulse ratio. This approach has caused much controversy because of the requirement of each pulse to form interference patterns in the same point of the light-sensitive material. However, this approach will certainly lead to a significant reduction in the printing speed. More importantly, by taking advantage of the pulsed coherent radiation, this method becomes insensitive to vibrations of the system.

In addition, it is worth mentioning that pulsed sources of coherent radiation are produced on the large potential volume of the holographic recording apparatus. However, the use of high power pulsed coherent radiation sources increases the power consumption of the device. All of these characteristics make it difficult to create compact holographic printers that use the continuous printing method.

4.2. Step-by-step printing method

In contrast to the continuous printing method, the step-by-step method involves the use of CW lasers as the coherent radiation source. However, the use of CW lasers requires a relatively long exposure time ranging from a few μs to tens or hundreds of *ms*. This does not allow for the recording of micro-holograms without stopping the light-sensitive material during the exposure.

#200122 - $15.00 USD Received 24 Oct 2013; revised 13 Dec 2013; accepted 15 Dec 2013; published 27 Jan 2014

As a result, the discontinuous movement of the material generates high levels of vibrations that cannot be ignored. In general, the time required for printing a synthetic hologram is determined by the diagram shown in Figure 2.

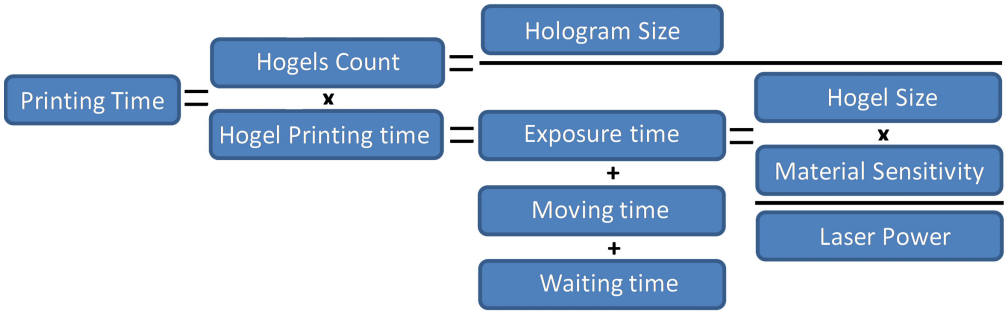

Fig. 2. Schematic diagram showing the printing time of the step-by-step method.

Using a symbolic representation, the time required to record one hogel is determined by

$$t_{hogel} = \tau + t_{move} + t_{wait}, \tag{8}$$

where τ, t_{move}, and t_{wait} represent the time required to expose one hogel, time required to move between two hogels, and waiting time after stopping the movement, respectively. Conversely, time required to expose one hogel according to [16] is determined by

$$\tau = d^2 \frac{S}{P\varepsilon}, \tag{9}$$

where d, S, P, and ε respectively represent the hogel size, sensitivity of the material, laser output power, and efficiency of the optical system.

The time required to move the light-sensitive material a distance equal to the hogel size for a constant acceleration is determined by

$$t_{move} = 2\sqrt{\frac{d}{a}}, \tag{10}$$

where a is the acceleration. [17]

When we take into account Eqs. (8), (9), and (10) as well as the diagram shown in Figure 2, the total time required to print an entire synthesized hologram is

$$T = \frac{A}{d^2}\left(d^2 \frac{S}{P\varepsilon} + 2\sqrt{\frac{d}{a}} + t_{wait}\right). \tag{11}$$

The waiting time, the time required for the movement to finish and then start the exposure again, is dependent on the mechanical stability and rigidity of the entire device, as well as the single hogel exposure time. Table 2 shows the results of the printing speed test for different exposure times, wavelengths, movement speeds, and waiting times. The principle experimental scheme shown in Figure 3 [18]. A two coordinate translating stage (*Micos Scan Table MS-8*) with DC motors was used as a mechanical positioner. We used three DPSS lasers, separate for each color. All experiments were carried outed by using of Bayer Bayfol HX-102 photopolymer material. It should be noted that the waiting time for a red wavelength of light was nearly 5

#200122 - $15.00 USD Received 24 Oct 2013; revised 13 Dec 2013; accepted 15 Dec 2013; published 27 Jan 2014

times less than that for green and blue wavelengths. In addition, the blue wavelength had a much lower acceleration compared to the red and green wavelengths.

This reduction in waiting time for the red wavelength is primarily because the exposure time for the green and blue was 10 and 8 ms respectively. In addition, in order to achieve the same hogel to hogel uniformity for the same green and blue waiting time, the exposure time for the blue wavelength must to less than that of the green one. This is because of the higher vibration sensitivity of the blue grating, which is a consequence of the high spatial frequency of the formed interference pattern.

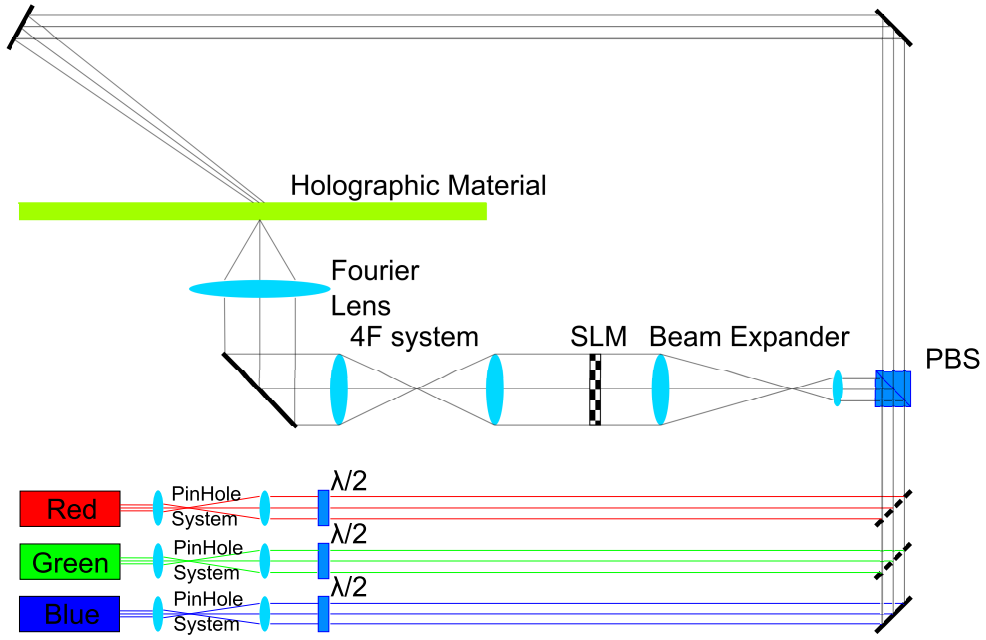

Fig. 3. Principle optical scheme of experimental optical setup used for hogel printing time testing.

Table 2. Results of the printing speed test.

Laser	Red	Green	Blue
Wavelength (*nm*)	671	532	473
Actual laser power (*mW*)	240	100	180
Exposure dosage ($\frac{mJ}{cm^2}$)	4	16	24
Exposure time (*ms*)	1	10	8
Hogel size (*mm*)	1.8	1.8	1.8
Moving time (*ms*)	115	225	225
Acceleration ($\frac{mm}{s^2}$)	550	150	150
Waiting time (*ms*)	25	115	115
Time per hogel (*ms*)	141	350	348
Total time for D4 (*min*)	9.5	23.6	23.5
Hogel to hogel uniformity (%)	90	85	82.5

#200122 - $15.00 USD Received 24 Oct 2013; revised 13 Dec 2013; accepted 15 Dec 2013; published 27 Jan 2014

4.3. As intermediate conclusion

Table 3 shows the advantages and disadvantages of the considered holographic printing methods. As shown in Table 3, the major disadvantages of the step-by-step method include the following: a high vibration sensitivity, long exposure time, and potentially slow printing speed. Let us examine different techniques to reduce these problems.

Table 3. Comparison of the pulse and step-by-step holographic printing methods.

Item	Pulse		Step-by-step	
Vibration sensitivity	Low	+	High	−
Used material	Silver Halide	−	Photopolymer	+
Typical exposure time	*ns*	+	*ms*	−
Used lasers	Pulsed	−	CW	+
Potential device size	Big	−	Small	+
Potential printing speed	High	+	Middle	−

The *Vibration sensitivity* may be reduced by using a more compact arrangement and lighter mechanical parts with a higher rigidity. One way to reduce the vibration influence is by the use of compact and inflexible optical parts, e.g., something similar to the integral optical recording device discussed in [19], Kyungsuk Pyun et al.

Meanwhile, the material *exposure time* may be reduced by using more powerful coherent light sources. However, this will cause the device size and power consumption to increase. An alternative solution to this problem can be increasing the optical efficiency because the exposure time is inversely proportional to the optical efficiency as shown in Eq. (9). In [19], Pyun et al. proposed the use of an integral optical module that is compact, inflexible, and has a high optical efficiency.

The *printing speed* depends on several factors. However, the factor that likely affects the printing speed the most is the waiting time. It is important that a moving material have a sufficient waiting time so that the vibration level can be sufficiently reduced (see Figure 2). A possible solution to the printing speed problem is the use of a multi-printing head. However, this method increases the overall device size as well as the number of coherent light sources. One of more the interesting ways to overcome the printing speed is to print several hogels at the same position of light sensitive material. This is called multi-hogel printing technology.

5. Multi-hogel printing technology

Simultaneous printing of several hogels can be achieved using different methods, which is split into two main groups:

I Spatial splitting;

II Time sequential.

Methods belonging to Group **I** record all hogels in a hogel cluster at the same time. However, during the recording, spatial splitting of its angular spectrum occurs due to multiple hogels sharing the single spatial light modulator (SLM) information. This approached reduces the image quality when compared to the conventional printing method (single hogel printing method). Conversely, methods belong to Group **II** form images that are separated by time and spatial hogels at a fixed position on the light sensitive material. At the same time, the entire SLM resolution is used to form an angular spectrum of each hogel. In that case, it is possible to achieve the same image quality as the single hogel printing method.

#200122 - $15.00 USD Received 24 Oct 2013; revised 13 Dec 2013; accepted 15 Dec 2013; published 27 Jan 2014

5.1. *Efficiency of multi-hogel printing technology*

In order to estimate the efficiency of the simultaneously printing methods of several hogels, we modify Eq. (11) to

$$T = A\frac{S}{P\varepsilon} + 2K\sqrt{\frac{d}{a}} + t_{wait}K. \tag{12}$$

The first item on the right hand side of the equal sign is the total exposure time or the time required to expose the entire printing area. It is evident from Eq. (11) that the total exposure time is independent of a single hogel size. Therefore, the exposure time is constant for a fixed laser power and optical system. Moreover, all the other terms in Eq. (12) are directly proportional to the total number of steps that are required to cover the entire printing area, i.e., for the case of single hogel printing this corresponds to the number of hogels in a printed image. The total number of hogels can be calculated using $K = \frac{A}{d^2}$.

Since most of the Fourier transforming objective lenses are axially symmetric, they form a circular line field in the back focal plane. Therefore, if hogel shape is square and all hogels are distributed along a rectangular grid, it is evident that the optimal placement of the hogels in the hogel cluster exhibits the same shape as the single hogel within the accuracy of the scale. As such, each hogel cluster will contain M^2 single hogels, where M is positive integer greater than 1.

Let us rewrite Eq. (12) by taking into account the number of hogels in one hogel cluster

$$T = A\frac{S}{P\varepsilon} + 2K\sqrt{\frac{dM}{a}} + t_{wait}K, \tag{13}$$

where the total number of steps K are defined as $K = \frac{A}{d^2M^2}$. As Eq. (13) shows, the total waiting time of the system is reduced by M^2 when compared to the single hogel printing method. At the same time, the overall moving time is reduced by [20] $M^{3/2}$.Furthermore, Eq. (13) describes a method from Group **I**.

Meanwhile, the total printing time for Group **II** can be defined as

$$T = A\frac{S}{P\varepsilon} + 2K\sqrt{\frac{dM}{a}} + t_{wait}K + K(M^2-1)t_{shift}, \tag{14}$$

where t_{shift} represents the time required for the optical system to print the next hogel in hogel cluster. For the ideal case, $t_{shift} = {f_{SLM}}^{-1}$, where f_{SLM} represents the SLM frame rate.

6. Spatial Splitting Technology

Now, we consider the limitations imposed on the construction of the optical part of the printing head that is configured for the simultaneous printing of several hogels using the spatial splitting of their angular spectra. There are many possible designs for achieving spatial the splitting of multi-hogel printing technology. Hereafter, we will consider the design described by Putilin et al. [21]. This scheme uses a pair of pyramidal optical wedges to produce the spatial splitting of the angular spectra for different hogels in a hogel cluster. The main setup of such a device is shown in Figure 4.

In general, the field of view of a synthesized holographic image is defined by a single hogel field of view according to [6] using

$$2\sigma = 2\arctan\frac{h}{2f}, \tag{15}$$

where 2σ, h, and f represent the entire angle defined for a single hogel field of view, linear size of a SLM placed at front of the focal plane of Fourier transforming optical system, and

#200122 - $15.00 USD Received 24 Oct 2013; revised 13 Dec 2013; accepted 15 Dec 2013; published 27 Jan 2014

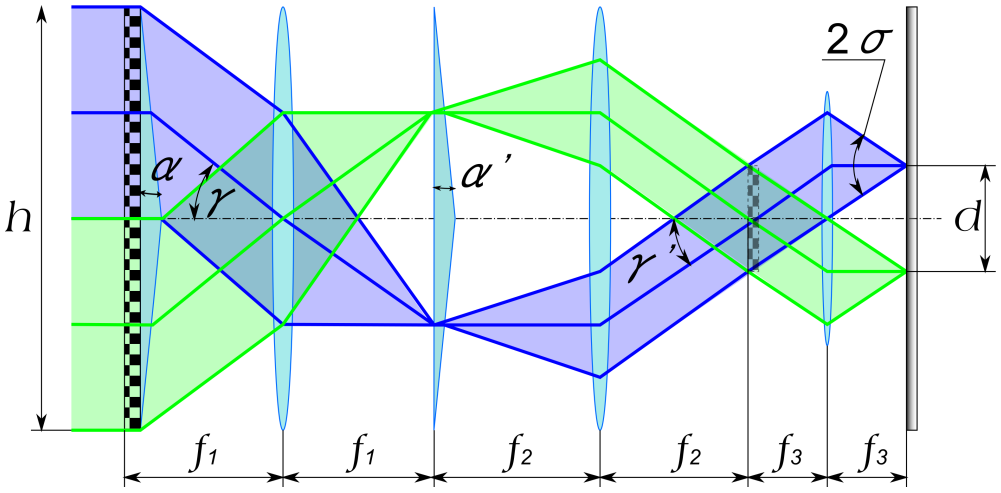

Fig. 4. Schematic diagram showing the operational principle of the bi-wedge based multi-hogel printing setup.

focal distance of a Fourier transforming optical system, respectively. Meanwhile, the numerical aperture of the this optical Fourier transforming system (according to [6]) can be described using

$$NA = \sin\left(\arctan\frac{D}{2f}\right) \approx \sin\left(\arctan\frac{h}{2f}\right) = \sin\sigma, \tag{16}$$

where D is the diameter of the Fourier transforming optical system exit pupil.

For the optical system shown in Figure 4, the field of view is defined as

$$2\sigma = 2\arctan\frac{h}{2Mf_\Sigma}, \tag{17}$$

where M is positive integer greater than 1, M^2 is the number of hogels in one hogel cluster (see Section 5), and f_Σ is the total focal distance of the optical system. The total focal distance of such a system according to [6] can be defined as

$$\Phi_\Sigma = \Phi_1 + \Phi_2 + \Phi_3 - \Phi_1 d_1 (\Phi_2 + \Phi_3) - \Phi_3 d_2 (\Phi_1 + \Phi_2 - \Phi_1\Phi_2 d_1), \tag{18}$$

where $\Phi_\Sigma = 1/f_\Sigma$ is the optical power of the whole optical system, $\Phi_1 = 1/f_1$ is the optical power of the first component, $\Phi_2 = 1/f_2$ is the optical power of the second component, $\Phi_3 = 1/f_3$ is the optical power of the third component, $d_1 = f_1 + f_2$ is the distance between first and second components, and $d_2 = f_2 + f_3$ is the distance between the second and third components.

Taking into account Eq. (18), we can rewrite Eq. (17) as

$$2\sigma = 2\arctan\frac{hf_2}{2Mf_3f_1}. \tag{19}$$

#200122 - $15.00 USD Received 24 Oct 2013; revised 13 Dec 2013; accepted 15 Dec 2013; published 27 Jan 2014

By comparing Eqs. (15) and (17) and taking into account Eq. (19), we find the following: [22]

$$f_\Sigma = \frac{f_1 f_3}{f_2} = \frac{f}{M}. \tag{20}$$

Thus, the effective focal distance of a system with spatial splitting of the angular spectra of different hogels should be in M times less than that of a single hogel printing optical system. We can define the numerical aperture for this case using of Eqs. (16) and (20)

$$NA_\Sigma = \sin\left(\arctan\frac{hM}{2f}\right). \tag{21}$$

Notice that the numerical aperture of the Fourier transforming systems with spatial splitting of the angular spectra of separate hogels increase as the number of hogels in a hogel cluster increases. This causes a reduction in the synthesized image field of view. Table 4 shows dependency of the field of view and numerical aperture on the number of hogels in a hogel cluster [23]. Additionally, notice that the maximum Fourier objective numerical value can only provide a maximum field of view of 60°.

Table 4. Table showing dependence of the field of view and required Fourier objective NA on the number of hogels in a hogel cluster for a spatial splitting multi-hogel system.

M^2	1	4	9	16	25
Field of view, °	60	60	41.4	31.7	25.6
Required NA	0.5	0.76	0.87	0.92	0.94

When we split the SLM information space between several hogels, we reduce the information capacity of a single hogel. As result, the maximum achievable angular resolution of a synthesized hologram is reduced. In general, the synthesized hologram field of view is a cone containing a circular cone basis and an angle equal to the hogel field of view. The maximum achievable angular resolution for a hogel as a function of SLM resolution is [24]

$$\Delta\gamma = \frac{M\sigma}{\sqrt{\frac{N_\circ}{\pi}}} = \frac{2M\sigma}{\sqrt{N}}, \tag{22}$$

where N, $N_\circ = N\frac{\pi}{4}$, σ, and M^2, represent the SML pixel number, SLM pixel number used for forming the hogel field of view, half angle of a hogel's field of view, and number of hogels in a hogel cluster, respectively. We emphasize that Eq. (22) is valid only for f-Theta Fourier lenses. Table 5 shows the variation of the angular resolution as a function of M^2 for a VGA SLM holographic image formed by an f-Theta Fourier objective.

Table 5. Possible angular resolutions of a spatial splitting multi-hogel system as a function of the number of hogels in a hogel cluster for a VGA SLM formed by an f-Theta Fourier objective.

M^2	1	4	9	16	25
$\Delta\gamma$, °	0.125	0.25	0.375	0.5	0.625

If we use a conventional Fourier lens instead of an f-Theta one, Eq. (22) becomes

$$\Delta\gamma = \arctan\frac{2M\tan\sigma}{\sqrt{N}}, \tag{23}$$

#200122 - $15.00 USD Received 24 Oct 2013; revised 13 Dec 2013; accepted 15 Dec 2013; published 27 Jan 2014

where N, σ, and M^2 represent the SLM pixel number, half angle of a hogel's field of view, and number of hogels in a hogel cluster. Table 6 shows the variation of the angular resolution as a function of M^2 for a VGA SLM holographic image formed by a conventional Fourier objective. As one can see, spatial splitting technology can significantly reduce the printing time compared to the single hogel printing technology. However, serious limitations occur not only in the manufacturability but also in the image quality of the formed hologram.

Table 6. Possible angular resolutions of a spatial splitting multi-hogel system as a function of the number of hogels in a hogel cluster for a VGA SLM formed by a conventional Fourier objective.

M^2	1	4	9	16	25
$\Delta\gamma$, °	0.138	0.278	0.413	0.551	0.689

7. Time sequential Technology

The time sequential method allows us to keep the same information capacity of each hogel and is distinct from the technologies based on the spatial splitting of SLM information. A device based on such technology was first described by Putilin et al. [25]. The main design of a time sequential multi-hogel system is shown in Figure 5. This method is based on the usage of a

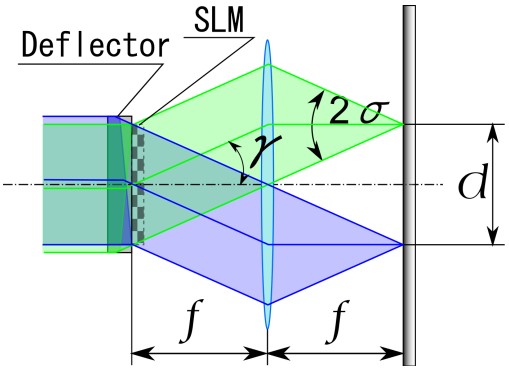

Fig. 5. Schematic diagram showing the main design of a time sequential multi-hogel system.

special optical beam deflector that deflects the beam at an angle γ. This angle defines the shift of recording hogel position according to [6] using

$$d = f \tan\gamma. \tag{24}$$

Meanwhile, the numerical aperture of the Fourier transformation objective can be defined as

$$NA = \sin\left(\arctan\frac{h+Md}{2f}\right), \tag{25}$$

where h, M, f, and d represent the SLM linear size, square root of the number of hogels in a hogel cluster, Fourier transformation lens focal distance, and shift of the hogel position that is equal to size of a single hogel in a hogel cluster, respectively.

The main advantage of this design is the fixed information capacity of each hogel as well as the angular resolution of a printed synthesized holographic image. When compared to devices

#200122 - $15.00 USD Received 24 Oct 2013; revised 13 Dec 2013; accepted 15 Dec 2013; published 27 Jan 2014

that are related to Group **I**, the main disadvantage of the time sequential scheme is the printing time of a single hogel increases because of the time required to deflect a passing beam using an optical deflector. However, for the case of an electro-optical deflector, the addition time is insignificant.

8. Comparison of different printing methods

Table 7 summarizes the advantages of the printing speed and results from the usage of multi-hogel technology at a fixed position in light-sensitive materials compared to conventional step-by-step printing. It should be noted that the information capacity and angular resolution of sep-

Table 7. Comparison between multi-hogel printing technology and conventional one.

Time	Conventional	Group **I**	Group **II**
Exposure	1	1	1
Moving	1	$M^{-3/2}$	$M^{-3/2}$
Waiting	1	M^{-2}	M^{-2}
Additional	0	0	$\frac{A}{d^2}\frac{M^2-1}{M^2}t_{shift}$

arately printed hogels from synthesized holographic images with an increasing Fourier transforming optical system complexity belong to Group **I**. The increase in the optical system complexity is due to the increasing hogel number in a hogel cluster. Thus, one cannot uniquely identify the optimal technology for each particular case.

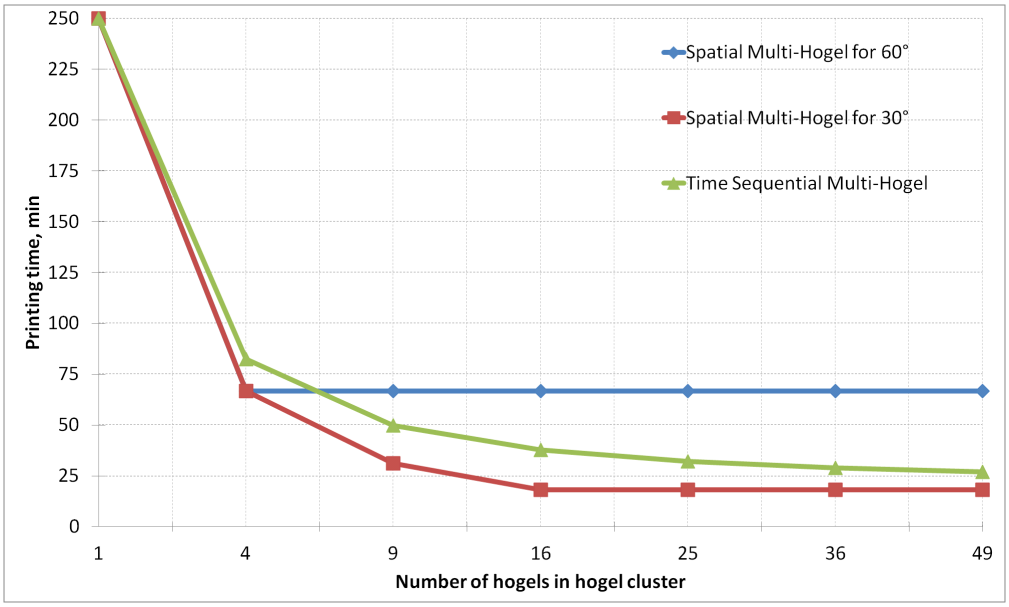

Fig. 6. Predicted printing time for spatial and time sequential multi-hogel systems.

Time required to print a synthesized holographic image with the following parameters is shown in Figure 6: [26] size, field of view, and single hogel size are $10 \times 10\ cm^2$, 60°or 30°, and $0.2\times\ 0.2mm^2$, respectively. It is clear that at large viewing angles (60°) the synthesized image using the spatial multi-hogel method containing 4 ($M = 2$) hogels has some advantages when

#200122 - $15.00 USD Received 24 Oct 2013; revised 13 Dec 2013; accepted 15 Dec 2013; published 27 Jan 2014

compared to the time sequential method. For a larger amount of hogels, the time sequential method is advantageous due to the fact that this system with SLM spatial splitting requires a numerical aperture greater than 0.76 and cannot form more than 4 hogels in a hogel cluster. In addition, the spatial multi-hogel has the narrowest field of view, i.e., approximately 30° field of view for time and spatial multi-hogels. Conversely, the time sequential design exhibited a narrow field of view for high M^2, i.e., more than 16. In fact, for $M^2 \geq 16$, there is no difference between the spatial and time multi-hogels. Therefore, the selection of holographic systems should be made based on economic considerations.

9. Conclusion

The investigation of the main factors that have an influence on the time of hologram synthesis was fulfilled in this research. The application of CW lasers makes more complicated the operation manner of mechanical translators, the time of delay between mechanical movement and exposure defines increasing overall recording time, so the parallel recording of several holels became actual. But at the same time the requirements of the quality of optical elements (especially, Fourier optics) of multi-hogel schemes became more strict. The modeling of several real experimental arrangements permit us to define the parameters of the arrangement required for decreasing of overall recording time. For example, for parameters of the schemes mentioned above, conventional printing method will takes 250 minutes to print one image with size $10 \times 10\ cm^2$. On the same time, spatial splitting technology allows to print four hogel in one time and reduce overall printing time till 67 minutes with small image quality reduction. The time sequential technology with 25 hogels in one hogel cluster will print same image just for 32 minutes without any image quality reduction.

Acknowledgments

This work was carried out as a part of the global collaboration work by Samsung Advanced Institute of Technology in collaboration with SAIT Russia Lab and Lebedev Physical Institute of Russian Academy of Science. We would like to acknowledge the Director of the SAIT Russia Lab, Mr. Sangyoon Oh, as well as the head of global project Dr. Kyungsuk (Peter) Pyun for their support. We would like to provide our regards to the members of this project from the Samsung Advanced Institute of Technology: Drs. Chilsung Choi, Sunil Kim, and Jungkweun An for their contribution. We are lucky to give our respects to Drs. Hongseok Lee and Sangyoon Lee.

#200122 - $15.00 USD Received 24 Oct 2013; revised 13 Dec 2013; accepted 15 Dec 2013; published 27 Jan 2014